

International Journal of Modern Physics D
 © World Scientific Publishing Company

PHOTON REGIONS AND SHADOWS OF ACCELERATED BLACK HOLES

ARNE GRENZEBACH*, VOLKER PERLICK† and CLAUD LÄMMERZAHL‡

*ZARM, University of Bremen,
 Am Fallturm, 28359 Bremen, Germany*

Received Day Month Year

Revised Day Month Year

In an earlier paper we have analytically determined the photon regions and the shadows of black holes of the Plebański class of metrics which are also known as the Kerr–Newman–NUT–(anti-)deSitter metrics. These metrics are characterized by six parameters: mass, spin, electric and magnetic charge, gravitomagnetic NUT charge, and the cosmological constant. Here we extend this analysis to the Plebański–Demiański class of metrics which contains, in addition to these six parameters, the so-called acceleration parameter. All these metrics are axially symmetric and stationary type D solutions to the Einstein–Maxwell equations with a cosmological constant. We derive analytical formulas for the photon regions (i.e., for the regions that contain spherical lightlike geodesics) and for the boundary curve of the shadow as it is seen by an observer at Boyer–Lindquist coordinates (r_O, ϑ_O) in the domain of outer communication. Whereas all relevant formulas are derived for the whole Plebański–Demiański class, we concentrate on the accelerated Kerr metric (i.e., only mass, spin and acceleration parameter are different from zero) when discussing the influence of the acceleration parameter on the photon region and on the shadow in terms of pictures. The accelerated Kerr metric is also known as the rotating C -metric. We discuss how our analytical formulas can be used for calculating the horizontal and vertical angular diameters of the shadow and we estimate these values for the black holes at the center of our Galaxy and at the center of M87.

Keywords: Black hole; acceleration; shadow.

PACS numbers: 04.70.-s, 95.30.Sf, 98.35.Jk

1. Introduction

Basically, the *shadow* of a black hole is the region on the observer’s sky that is left dark if the light sources are anywhere in the universe but not between the observer and the black hole. For a mathematical description, it is convenient to consider light rays that are sent from the observer’s position into the past. Some of them are deflected by the black hole and then go out to bigger radii again; because they

*arne.grenzebach@zarm.uni-bremen.de

†volker.perlick@zarm.uni-bremen.de

‡claus.laemmerzahl@zarm.uni-bremen.de

2 Arne Grenzebach, Volker Perlick, Claus Lämmerzahl

can reach one of the light sources, we assign brightness to their initial directions. Others stay close to the radial line and go to the horizon without meeting one of the light sources; to their initial directions we assign darkness. The resulting dark region on the sky is called the *shadow* of the black hole. The boundary of the shadow is determined by light rays that spiral towards a lightlike geodesic which stays on a sphere. The region outside of the black hole filled with these spherical lightlike geodesics is called the exterior *photon region*. Recently, the shadow of a black has attracted even Hollywood's attention. In the movie *Interstellar*, which was released in 2014, it was shown how nearby observers would see the shadow of an almost extremal rotating (Kerr) black hole with an accretion disk.²

In the near future astronomers actually expect to observe the shadow of a black hole. Currently there are two cooperating projects—the US-led Event Horizon Telescope project³ and the European BlackHoleCam project—who try to image the shadow of galactic black holes. It has been predicted since several years that there are supermassive black holes at the centers of most—if not all—galaxies. There is strong evidence for a black hole at the center of our own Galaxy, associated with the radio source Sagittarius A* (Sgr A*): Infrared observations of orbits of stars near the center^{4,5} demonstrate that there has to be a heavy object with a mass of approximately 4.3 million Solar masses within a small volume. The most convincing candidate for such an object is a black hole. Another good candidate for a supermassive black hole is the object at the center of M87 ($m > 10^9$ Solar masses). Because of the large distance, the diameter of the shadow of galactic black holes will be tiny. Even for the nearest candidate Sgr A* (8.3 kpc away^{5,6}), the predicted diameter of the shadow is only about 50 microarcseconds, see Sec. 5. Although tiny, such a diameter should be resolvable with very large baseline interferometry (VLBI).^{3,7} Numerical studies taking scattering into account suggest that the shadow can be observed only at sub-millimeter wavelengths, see Falcke, Melia and Agol.⁸ The resolution of interferometric measurements in this wavelength regime will be further improved if the 10-meter space-based radio-telescope *Millimetron*⁹ goes into operation, probably in the mid-2020s. With this Russian satellite the Earth-based telescope network is upgraded with an extra-long Space-Earth baseline of 1.5 million km.

If the shadow of a black hole will be observed, its shape will give important information on the parameters of the black hole. Therefore, it is necessary to provide the observers with theoretical calculations of the shape of the shadow for different black-hole models. In an earlier paper,¹ we have given an analytic formula for the shadow of black holes of the Plebański class, which are also known as Kerr–Newman–NUT–(anti-)de Sitter space-times. Black holes of this class are characterized by mass, spin, electric or magnetic charge, a NUT-parameter and a cosmological constant. In the present paper we extend this analysis to the bigger class of Plebański–Demiański space-times, which include in addition a so-called acceleration parameter. The Plebański–Demiański space-times are axially symmetric stationary solutions to the Einstein–Maxwell equations with a cosmological constant and they are of Petrov type D. Before determining the boundary curve of the shadow

in these space-times, we have to study the photon region. We develop the relevant formulas for the whole class of Plebański–Demiański space-times. However, when studying the effect of the acceleration parameter onto the photon region and onto the shadow in terms of pictures, we restrict to black holes for which only the mass, the spin and the acceleration parameter are different from zero. This is because the effect of the other parameters – electric and magnetic charge, NUT-parameter and cosmological constant – has been studied already in our earlier paper and the presence of the acceleration does not change this significantly. The metric of these black hole space-times characterized by mass, spin and acceleration alone is known as the rotating C -metric or the accelerated Kerr metric.

If only the mass and the acceleration parameter are different from zero, we have the so-called C -metric which describes a space-time with boost-rotation symmetry. This solution to the vacuum Einstein field equation was found by Levi-Civita (1919)¹⁰ and Weyl (1919).^{11,12} The name C -metric refers to the classification in the review of Ehlers and Kundt (1962).¹³ The rotating version of the C -metric was considered by Hong and Teo¹⁴ while a detailed discussion of accelerated space-times in general can be found in the book by Griffiths and Podolský.¹⁵

Commonly the C -metric is given in the form introduced by Hong and Teo¹⁶

$$g_{\mu\nu}^C dx^\mu dx^\nu = \frac{1}{\alpha^2(x+y)^2} \left(-F d\tau^2 + \frac{dy^2}{F} + \frac{dx^2}{G} + G d\varphi^2 \right) \quad (1)$$

with cubic functions $G = (1-x^2)(1+2\alpha m x)$ and $F = -(1-y^2)(1-2\alpha m y)$. The metric depends on two parameters, the mass m and the acceleration parameter α . The domain covered by the coordinates (τ, x, y, φ) actually contains *two* black holes accelerating away from each other with a conical singularity (a “strut”) on the axis of rotational symmetry.^{15,17–19} For our purposes, Boyer–Lindquist coordinates are more suitable, see Eq. (2) below, which cover only one of the two black holes.

There are several earlier papers on the shadows of black holes. Here we just mention some important works, for a more comprehensive list we refer to the introduction of our earlier paper.¹ The first analytic calculations of the shadow of a black hole were done by Synge²⁰ for the Schwarzschild metric (Synge used the word “escape cone” for the complement of the shadow) and by Bardeen²¹ for the Kerr metric. In the Schwarzschild case the photon region reduces to the “photon sphere” at $r = 3m$ and the shadow is circular. In the Kerr case, the photon region is spatially three-dimensional and the shadow is non-circular. The deviation of the shadow from a circle could be used as a measure for the spin.²² With ray-tracing algorithms it is possible to include effects of matter on the light rays like emission regions and scattering.^{23–29} Here we do not take such effects into account but restrict ourselves to the purely geometric construction of the shadow based on the assumption that light rays are lightlike geodesics and that there are no light sources between us and the black hole. It is our goal to derive an analytical formula for the shape of the shadow from which, in future work, the parameters of the black hole could be extracted with analytical means.

4 Arne Grenzebach, Volker Perlick, Claus Lämmerzahl

After a discussion of relevant properties of the Plebański–Demiański space-times (Sec. 2) we determine the photon region (Sec. 3) which is essential for calculating the boundary of the shadow of the black hole for an observer at Boyer–Lindquist coordinates (r_O, ϑ_O) (Sec. 4). We derive all relevant formulas for the whole Plebański–Demiański class. However, when illustrating the results with pictures of the photon region and of the shadow in Secs. 3 and 4 we restrict to the accelerated Kerr metric. In Sec. 5 we discuss how our analytical formulas can be used for calculating the angular diameters of the shadow. We use these equations for estimating the angular diameters of the shadows of Sgr A* and M87.

2. The Plebański–Demiański metrics

We consider the general Plebański–Demiański class of stationary, axially symmetric type D solutions of the Einstein–Maxwell equations with a cosmological constant. As a matter of fact, these solutions were first found by Debever³⁰ in 1971 but are better known in the form of Plebański and Demiański³¹ from 1976. The Plebański–Demiański metrics are discussed in detail by Griffiths and Podolský¹⁵ and by Stephani et al.³² It is common to use rescaled units, i.e. units so that the speed of light and the gravitational constant are normalized ($c = 1$, $G = 1$). In Boyer–Lindquist coordinates this metric is then given by, see Ref. 15, p. 311

$$g_{\mu\nu} dx^\mu dx^\nu = \frac{1}{\Omega^2} \left(\Sigma \left(\frac{1}{\Delta_r} dr^2 + \frac{1}{\Delta_\vartheta} d\vartheta^2 \right) + \frac{1}{\Sigma} \left((\Sigma + a\chi)^2 \Delta_\vartheta \sin^2 \vartheta - \Delta_r \chi^2 \right) d\varphi^2 \right. \\ \left. + \frac{2}{\Sigma} \left(\Delta_r \chi - a(\Sigma + a\chi) \Delta_\vartheta \sin^2 \vartheta \right) dt d\varphi - \frac{1}{\Sigma} \left(\Delta_r - a^2 \Delta_\vartheta \sin^2 \vartheta \right) dt^2 \right) \quad (2)$$

with the abbreviations

$$\begin{aligned} \Omega &= 1 - \frac{\alpha}{\omega} (\ell + a \cos \vartheta) r, & \Delta_\vartheta &= 1 - a_3 \cos \vartheta - a_4 \cos^2 \vartheta, \\ \Sigma &= r^2 + (\ell + a \cos \vartheta)^2, & \Delta_r &= b_0 + b_1 r + b_2 r^2 + b_3 r^3 + b_4 r^4. \end{aligned} \quad (3)$$

The coefficients of the polynomials Δ_ϑ and Δ_r are

$$\begin{aligned} a_3 &= 2 \frac{\alpha}{\omega} a m - 4 a \ell \left(\frac{\alpha^2}{\omega^2} (k + \beta) + \frac{\Lambda}{3} \right), \\ a_4 &= -a^2 \left(\frac{\alpha^2}{\omega^2} (k + \beta) + \frac{\Lambda}{3} \right), \end{aligned} \quad (4)$$

$$\begin{aligned} b_0 &= k + \beta, \\ b_1 &= -2m, \\ b_2 &= \frac{k}{a^2 - \ell^2} + 4 \frac{\alpha}{\omega} \ell m - (a^2 + 3\ell^2) \left(\frac{\alpha^2}{\omega^2} (k + \beta) + \frac{\Lambda}{3} \right), \\ b_3 &= -2 \frac{\alpha}{\omega} \left(\frac{k\ell}{a^2 - \ell^2} - (a^2 - \ell^2) \left(\frac{\alpha}{\omega} m - \ell \left(\frac{\alpha^2}{\omega^2} (k + \beta) + \frac{\Lambda}{3} \right) \right) \right), \\ b_4 &= - \left(\frac{\alpha^2}{\omega^2} k + \frac{\Lambda}{3} \right) \end{aligned} \quad (5)$$

with

$$k = \frac{1 + 2\frac{\alpha}{\omega}\ell m - 3\ell^2\left(\frac{\alpha^2}{\omega^2}\beta + \frac{\Lambda}{3}\right)}{1 + 3\frac{\alpha^2}{\omega^2}\ell^2(a^2 - \ell^2)}(a^2 - \ell^2), \quad \omega = \sqrt{a^2 + \ell^2}. \quad (6)$$

Basically, the coordinates t and r may range over all of \mathbb{R} while ϑ and φ are standard coordinates on the two-sphere. Note, however, that for some values of the black-hole parameters r and ϑ have to be restricted, see below. The Plebański–Demiański space-time depends on seven parameters, m , a , β , ℓ , α , Λ and C , which are to be interpreted in the following way. m is the mass of the black hole and a is its spin. β is a parameter that comprises electric and magnetic charge, $\beta = q_e^2 + q_m^2$, if non-negative; if β is negative, the metric cannot be interpreted as a solution to the Einstein–Maxwell equations but metrics of this form occur in some brane-world scenarios.³³ The NUT parameter ℓ is to be interpreted as a gravitomagnetic charge. The parameter α gives the acceleration of the black hole which is at the center of our investigation while Λ is the cosmological constant. The parameter C , which was introduced by Manko and Ruiz,³⁴ is relevant only if $\ell \neq 0$. In this case there is a (conic) singularity somewhere on the z axis and by choosing C appropriately this singularity can be distributed symmetrically or asymmetrically on the positive and the negative z axis. Note that this parameter C has nothing to do with the name “ C -metric” for the accelerated Schwarzschild space-time. All the parameters, m , a , ℓ , β , Λ , α and C , may take arbitrary real values in principle, albeit not all possibilities are physically relevant.

If $\alpha = 0$, the Plebański–Demiański class reduces to the Plebański space-times³⁵ which are also known as the Kerr–Newman–NUT–(anti-)de Sitter space-times. For this more special class of metrics the photon regions and the shadows have been discussed in our earlier paper, see Ref. 1. The Plebański–Demiański class covers many well-known non-accelerated ($\alpha = 0$) space-times like the Schwarzschild ($a = \beta = \ell = \Lambda = 0$), Kerr ($\beta = \ell = \Lambda = 0$), or Reissner–Nordström space-time ($a = \ell = \Lambda = 0$) as well as the accelerated C -metric ($a = \beta = \ell = \Lambda = 0$) or their rotating version ($\beta = \ell = \Lambda = 0$) which we will call *accelerated Kerr space-time*.

The metric (2) becomes singular at the roots of Ω , Σ , Δ_r , Δ_ϑ and $\sin\vartheta$. Some of them are mere coordinate singularities while others are true (curvature) singularities. In the following we briefly discuss the influence of α on these singularities.

Ω becomes zero if

$$r = \frac{\sqrt{a^2 + \ell^2}}{\alpha(\ell + a \cos\vartheta)}. \quad (7)$$

As the metric blows up if $\Omega \rightarrow 0$, Eq. (7) determines the boundary of the space-time, i.e., we have to restrict to the region where Ω is positive. The allowed region is a half-space bounded by a plane ($\ell = 0$), a half-space bounded by one sheet of a two-sheeted hyperboloid ($\ell^2 < a^2$), a domain bounded by a cylinder ($\ell^2 = a^2$), or a domain bounded by an ellipsoid ($\ell^2 > a^2$), see Fig. 1. For $\alpha = 0$ there is no restriction because $\Omega \equiv 1$.

6 Arne Grenzebach, Volker Perlick, Claus Lämmerzahl

Σ becomes zero at the ring singularity

$$r = 0 \quad \text{and} \quad \cos \vartheta = -\ell/a. \quad (8)$$

It exists for $\ell^2 < a^2$ and is a curvature singularity (if $m \neq 0$). Outside of this singularity the sphere $r = 0$ is regular, so it is possible to travel through one of these two hemispheres (“throats”) from the region $r > 0$ to the region $r < 0$ and vice versa. If $\ell^2 > a^2$, there is no ring singularity and the sphere $r = 0$ is regular everywhere. In the limiting case where $\ell^2 = a^2$ the ring singularity degenerates into a point on the axis. It becomes a point singularity for $\ell = a = 0$ that disconnects the space-time into the regions $r > 0$ and $r < 0$. The ring singularity is unaffected by α .

Moreover, the metric is singular on the z axis, i.e. if $\sin \vartheta = 0$. If $\alpha \neq 0$ oder $\ell \neq 0$, this is a true (conical) singularity on (at least a part of) the rotational axis. In the NUT case the singularity depends on the Manko-Ruiz parameter C . For further details we refer to the book by Griffiths and Podolský.¹⁵

The real roots of Δ_r yield coordinate singularities which correspond to the up to 4 horizons $r_1 > r_2 > \dots$ of the space-time. If $\alpha = 0$ and $\Lambda = 0$, then Δ_r reduces to a second-degree polynomial, $\Delta_r = r^2 - 2mr + a^2 - \ell^2 + \beta$, and horizons can be found at

$$r_{\pm} = m \pm \sqrt{m^2 - a^2 + \ell^2 - \beta} \quad (9)$$

if $a^2 \leq a_{\max}^2 := m^2 + \ell^2 - \beta$; then r_+ ($= r_1$) is the outer (event) horizon of the black hole and r_- ($= r_2$) is the inner horizon. The *domain of outer communication* is the region outside of the outer horizon where $\Delta_r > 0$. For $a^2 > a_{\max}^2$ we would find, instead of a black hole, a naked singularity or a regular space-time. Since we are interested only in the black hole case, we will not consider this possibility in the following. In the accelerated or cosmological scenario ($\alpha \neq 0$ or $\Lambda \neq 0$) the horizons could not in general be specified in a simple form because Δ_r is then a polynomial of degree 4. Depending on the sign of the leading coefficient b_4 , which is mostly determined by whether $a^2 > \ell^2$ and by the sign of Λ , the vector field ∂_r is timelike or spacelike for big values of r , see Fig. 1. In the timelike case (left column in Fig. 1), all real roots of Δ_r are in the allowed region with $\Omega > 0$. Hence, the first root r_1 represents a cosmological horizon and the subsequent root r_2 is the black-hole horizon. In this case the domain of outer communication is the region between r_1 and r_2 where $\Delta_r > 0$ (gray shaded and hatched region in Fig. 1). In the case that ∂_r is spacelike for big r (right column in Fig. 1), the first root r_1 is not in the allowed region. Hence, we have at r_2 a cosmological horizon, at r_3 the event horizon of the black hole, and in between the outer domain of communication. The horizons can be easily determined if $\beta = \ell = \Lambda = 0$. Then $k = a^2$ and $\omega = a$, hence

$$\Delta_r = (r^2 - 2mr + a^2)(1 - \alpha^2 r^2) \quad (10)$$

and we find the usual (Kerr) horizons at $r = r_{\pm}$ given by (9) with $\ell = 0$ and $\beta = 0$, and the additional horizons at $r = \pm \frac{1}{\alpha}$. Of course, we must have $|\alpha| < \frac{1}{r_{\pm}}$.

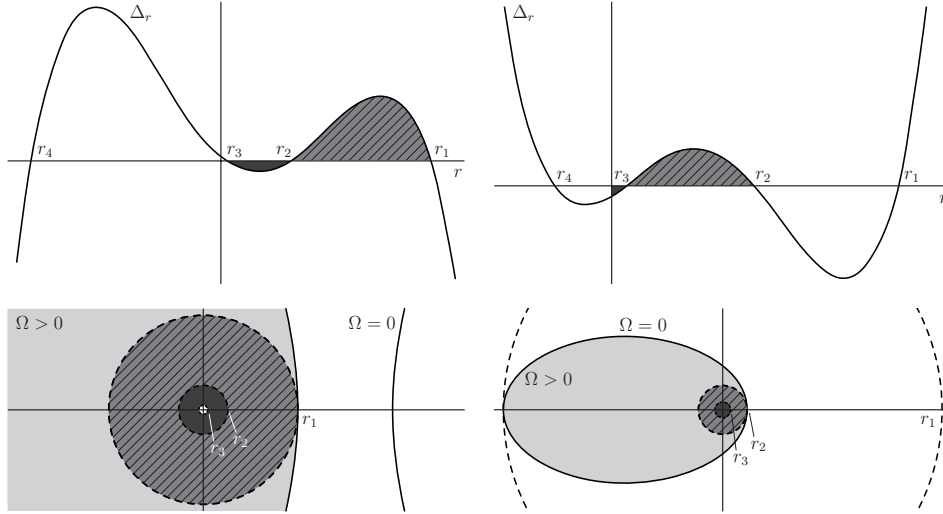


Fig. 1. A schematic illustration of the graph of Δ_r (upper row) and a polar plot of the region $\Omega > 0$ (lower row) given by (7). Depending on the sign of the leading coefficient b_4 , see (5), Δ_r goes to $+\infty$ or $-\infty$ for big radii r ; the space-times (with $\Lambda \geq 0$) belonging to the plots in the left column are dominated by the Kerr property ($\ell^2 < a^2$) and in the right column by the NUT property ($a^2 < \ell^2$). The space-time is restricted to that region where $\Omega > 0$ which is marked here with a light gray shading. Geometrically, the boundary of this region is one sheet of a two-sheeted hyperboloid (left) or an ellipsoid (right). As in the NUT dominated case (right) the root r_1 of Δ_r is not inside the allowed ellipsoid $\Omega > 0$, it could be no event horizon. Thus, the event horizon of the black hole is instead at r_3 (right) or at r_2 (left). The gray-shaded and hatched region marks the outer domain of communication ($\Delta_r > 0$) where we will place the observers.

In general, at the roots of Δ_ϑ would be coordinate singularities, too; these would indicate further horizons where the vector field ∂_ϑ would change the causal character from spacelike to timelike, just as the vector field ∂_r does at the roots of Δ_r . However, since these horizons would lie on cones $\vartheta = \text{constant}$ instead of on spheres $r = \text{constant}$ such a situation would be hardly of any physical relevance. Therefore, we exclude it by limiting the parameters of the black hole appropriately. As $\Delta_\vartheta = 0$ implies

$$\cos \vartheta_\pm = \frac{-a_3 \pm \sqrt{a_3^2 + 4a_4}}{2a_4}, \quad (11)$$

$\Delta_\vartheta \neq 0$ is guaranteed for all real ϑ if the radicand in (11) is negative. Therefore, we agree to choose the black-hole parameters such that $0 > a_3^2 + 4a_4$. If $\beta = \ell = \Lambda = 0$, this condition can be simplified. Then $k = a^2$ and $\omega = a$, hence

$$\Delta_\vartheta = 1 - 2\alpha m \cos \vartheta + \alpha^2 a^2 \cos^2 \vartheta, \quad (12)$$

and $\Delta_\vartheta \neq 0$ is assured if

$$|\alpha| < \begin{cases} \frac{1}{2m} & \text{if } a = 0, \\ \frac{r_-}{a^2} = \frac{m - \sqrt{m^2 - a^2}}{a^2} & \text{if } a \neq 0 \end{cases} \quad (13)$$

8 Arne Grenzebach, Volker Perlick, Claus Lämmerzahl

There are some other interesting regions around a black hole characterized by the change of the causal character of the Killing vector fields ∂_t and ∂_φ .

In that region where ∂_t becomes spacelike, i.e. $g_{tt} > 0$, no observer can move on a t -line. Thus, any observer in this region has to rotate (in φ direction). This region with $g_{tt} > 0$ is known as the *ergosphere* or the *ergoregion*^a. An ergoregion only exists if $a \neq 0$. Note that at the horizons, i.e. at the roots of Δ_r , the metric coefficient $g_{tt} = -\frac{1}{\Omega^2 \Sigma} (\Delta_r - a^2 \Delta_\vartheta \sin^2 \vartheta)$ is positive. Hence, the horizons are always contained within the ergoregion. For $\alpha \neq 0$ or $\Lambda \neq 0$ there are “cosmological” horizons in addition to the black-hole horizons; then the ergoregion consists of several connected components. The boundary of (a component of) the ergoregion is always tangential to the horizon on the rotational axis, i.e. at $\vartheta = 0, \pi$.

If $a \neq 0$ or $\ell \neq 0$, there are regions where the Killing field ∂_φ becomes timelike, $g_{\varphi\varphi} = 0$. This indicates causality violation, because the φ -lines are closed timelike curves. For $\ell = 0$ the region where $g_{\varphi\varphi} = 0$ is completely contained in the domain where $r < 0$ and, thus, hidden behind the horizon for an observer in the domain of outer communication. In the case $\ell \neq 0$, however, there is a causality violating region in the domain of outer communication around the axial singularity.

In the following, we will only consider the black-hole case where we have at least one positive root of Δ_r . Observers will be placed in the domain of outer communication.

3. Photon Regions

In the Plebański class of space-times, i.e., for $\alpha = 0$, the geodesic equation is completely integrable; in addition to the obvious constants of motion, there is a fourth constant of motion, known as the Carter constant, which is associated with a second-rank Killing tensor. If $\alpha \neq 0$, instead of this Killing tensor we only have a conformal Killing tensor. This is sufficient to assure complete integrability for *lightlike* geodesics. The four constants of motion are the Lagrangian

$$\mathcal{L} = \frac{1}{2} g_{\mu\nu} \dot{x}^\mu \dot{x}^\nu, \quad \mathcal{L} = 0 \quad \text{for light}, \quad (14)$$

the energy E and the z -component L_z of the angular momentum

$$E := -\frac{\partial \mathcal{L}}{\partial \dot{t}} = -g_{\varphi t} \dot{\varphi} - g_{tt} \dot{t}, \quad L_z := \frac{\partial \mathcal{L}}{\partial \dot{\varphi}} = g_{\varphi\varphi} \dot{\varphi} + g_{\varphi t} \dot{t}, \quad (15)$$

and the Carter constant K , see Ref. 36, which is now associated only with a conformal Killing tensor. The Carter constant may be viewed as the separation constant for the r and the ϑ motion of lightlike geodesics. The four constants of motion allow

^aSome authors call only the intersection of the region where $g_{tt} > 0$ with the domain of outer communication the *ergoregion*. This is that part of the region $g_{tt} > 0$ which an outside observer would be able to see.

us to write the lightlike geodesic equation in separated first-order form,

$$\frac{\Sigma}{\Omega^2} \dot{t} = \frac{\chi(L_z - E\chi)}{\Delta_\vartheta \sin^2 \vartheta} + \frac{(\Sigma + a\chi)((\Sigma + a\chi)E - aL_z)}{\Delta_r}, \quad (16a)$$

$$\frac{\Sigma}{\Omega^2} \dot{\varphi} = \frac{L_z - E\chi}{\Delta_\vartheta \sin^2 \vartheta} + \frac{a((\Sigma + a\chi)E - aL_z)}{\Delta_r}, \quad (16b)$$

$$\left(\frac{\Sigma}{\Omega^2}\right)^2 \dot{\vartheta}^2 = \Delta_\vartheta K - \frac{(\chi E - L_z)^2}{\sin^2 \vartheta} =: \Theta(\vartheta), \quad (16c)$$

$$\left(\frac{\Sigma}{\Omega^2}\right)^2 \dot{r}^2 = ((\Sigma + a\chi)E - aL_z)^2 - \Delta_r K =: R(r). \quad (16d)$$

In order to derive an equation for the shadow of accelerated black holes, we proceed in the same way as for the Plebański space-times. As a first step, we have to determine the spherical lightlike geodesics, i.e., lightlike geodesics staying on a sphere $r = \text{constant}$. The region filled by these spherical geodesics is called the *photon region* \mathcal{K} . Mathematically, spherical orbits are characterized by $\dot{r} = 0$ and $\ddot{r} = 0$ which requires by (16d) that $R(r) = 0$ and $R'(r) = 0$. Thus

$$K_E = \frac{((\Sigma + a\chi) - aL_E)^2}{\Delta_r}, \quad K_E = \frac{4r((\Sigma + a\chi) - aL_E)}{\Delta'_r}, \quad (17)$$

where Δ'_r is the derivative of Δ_r with respect to r and K_E, L_E are abbreviations

$$K_E = \frac{K}{E^2}, \quad L_E = \frac{L_z}{E}. \quad (18)$$

After solving (17) for the constants of motion

$$K_E = \frac{16r^2 \Delta_r}{(\Delta'_r)^2}, \quad aL_E = (\Sigma + a\chi) - \frac{4r \Delta_r}{\Delta'_r}, \quad (19)$$

we can substitute these expressions into (16c). As the left-hand side of (16c) is non-negative, we find an inequality that determines the photon region

$$\mathcal{K}: (4r \Delta_r - \Sigma \Delta'_r)^2 \leq 16a^2 r^2 \Delta_r \Delta_\vartheta \sin^2 \vartheta. \quad (20)$$

Of course, the equality sign determines the boundary of the photon region.

Just as in the non-accelerated space-times^{1,37} for every point (r_p, ϑ_p) of \mathcal{K} there is a lightlike geodesic through (r_p, ϑ_p) that stays on the sphere $r = r_p$. The ϑ motion is an oscillation bounded by the boundary of \mathcal{K} while the φ motion given by (16b) might be rather complicated.

The stability of these spherical geodesic with respect to radial perturbations is determined by the sign of R'' ; a spherical geodesic at $r = r_p$ is unstable if $R''(r_p) > 0$, and stable if $R''(r_p) < 0$. From (16d) we get with (19)

$$\frac{R''(r)}{8E^2} \Delta_r'^2 = 2r \Delta_r \Delta_r' + r^2 \Delta_r'^2 - 2r^2 \Delta_r \Delta_r''. \quad (21)$$

A non-rotating black hole ($a = 0$) is surrounded by a *photon sphere*, rather than by a photon region, since the inequality (20) defining \mathcal{K} reduces to an equality

$$4r\Delta_r = (r^2 + \ell^2)\Delta'_r. \quad (22)$$

The best known example is the photon sphere at $r = 3m$ in the Schwarzschild space-time.

Because of the rotational symmetry it is convenient to plot a meridional section through space-time for illustrating the regions around a black hole. The resulting pictures, which are (r, ϑ) polar diagrams where ϑ is measured from the positive z -axis, are shown in Fig. 2. Each figure contains the photon region \mathcal{K} , where unstable and stable spherical light rays are distinguished according to (21), the horizons r_{\pm} of the black hole given as boundaries of the region where $\Delta_r \leq 0$, the ergoregion, the causality violating region, and the ring singularity.

The dashed circle marks the throats at the sphere $r = 0$. For viewing the whole range of the space-time, we use two different scales for the radial coordinate: In the inner region $r < 0$ (inside the sphere $r = 0$) the radial coordinate is plotted as $m \exp(r/m)$; this is continuously extended with $r + m$ in the outer region $r > 0$ (outside the sphere $r = 0$). By not plotting just the exponential of the Boyer–Lindquist coordinate r , as suggested by O’Neill,³⁸ we avoid a strong deformation of the outer part.

While our formulas apply to black holes of the entire Plebański–Demiański class, in the pictures we restrict to accelerated Kerr space-times ($\beta = \ell = \Lambda = 0$) because we want to focus on the effect of the acceleration. Fig. 2 comprises various images of photon regions \mathcal{K} for different spin and acceleration parameters, where the spin is varied in the rows and the acceleration in the columns. For the spin we choose fractions of the value for an extremal black hole $a = \lambda a_{\max}$ with $\lambda \in \{\frac{1}{50}, \frac{2}{5}, \frac{4}{5}, 1\}$ and $a_{\max} = m$, cf. (9) and (10). Although one would expect only very small acceleration parameters in reality, we choose relatively big values ($\alpha \in \{0, \frac{1}{8m}, \frac{1}{6m}, \frac{1}{4m}\}$) for a better illustration of the effects. For each of the three values of the acceleration the figure is compared with the ordinary Kerr case.

In the ordinary Kerr space-time ($\alpha = 0$), see the left half of the images in the columns of Fig. 2, we see two photon regions: one with unstable orbits in the exterior region of the black hole at $r > r_+$ and one in the interior region at $r < r_-$ which contains unstable orbits as well as stable ones. For spinning black holes the exterior photon region develops a crescent-shaped cross-section which grows with increasing spin a . The inner photon region consists of two parts divided by the ring singularity. Note that also in the rotating case there are circular photon orbits, namely at that five points on the boundary of \mathcal{K} which are tangent to a sphere $r = \text{constant}$: there are three circular photon orbits in the equatorial plane—two at the boundary of the exterior photon region and one at the boundary of the interior photon region—and two more off the equatorial plane at the boundary of the interior photon region where $r < 0$. Furthermore, we find the ergoregion containing the horizons of the black hole, and in the interior adjacent to the ring singularity a causality violating

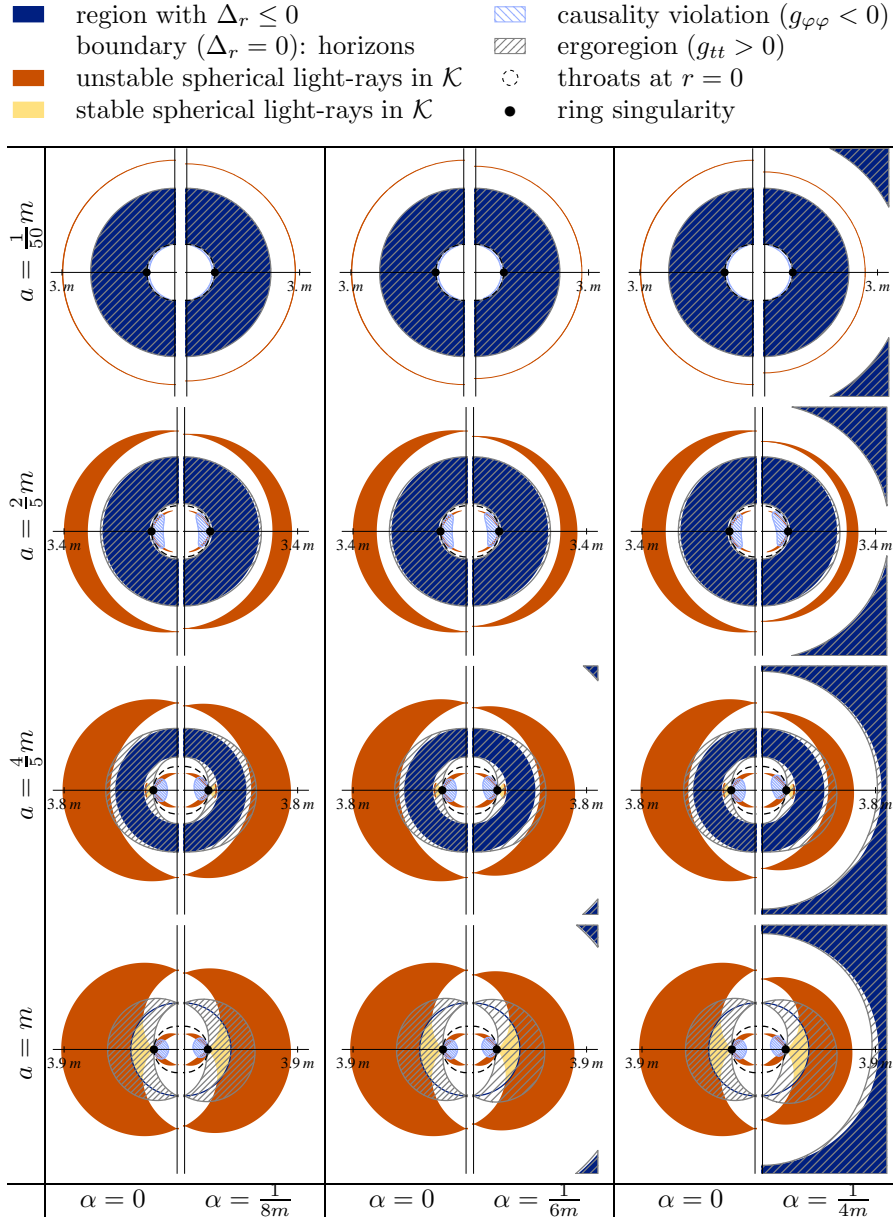


Fig. 2. Photon regions in accelerated Kerr space-time for spins $a = \lambda a_{\max}$, where $a_{\max} = m$. In each column the plot for the unaccelerated Kerr space-time (left) is compared to the plot for an accelerated Kerr space-time (right). The specific acceleration parameters are listed in the bottom row. A legend for the plotted regions is given at the top.

region. If $a^2 > m^2/2$ the ergoregion intersects the exterior photon region. All of these regions are symmetric with respect to the equatorial plane.

The plots for the accelerated Kerr space-times look similar to the non-accelerated ones but there are two significant differences. Firstly, a non-zero acceleration parameter gives rise to additional horizons, similarly to a cosmological constant. Secondly, the plots are no longer symmetric with respect to the equatorial plane which is similar to the NUT case. The additional outer horizon, a cosmological one, is best seen in the illustration for the highest acceleration $\alpha = \frac{1}{4m}$. In principle, such a horizon also appears in all other plots but most or even all of it is located outside of the shown clipping. The asymmetry with respect to the equatorial plane is best seen for $\alpha = \frac{1}{4m}$. With the exception of the causality violating region, the entire picture looks as if pushed into the negative z direction, i.e., into the direction against the direction of the acceleration. For a better view, Fig. 3 shows bigger versions of the two plots shown in the fourth row of the third column in Fig. 2.

As one would expect, the photon region, the ergoregion and the causality violating region depend on the signs of a and α . While the photon region is reflected at the equatorial plane if the sign of α is changed, the ergoregion and the causality violating region are reflected if the sign of $a\alpha$ is changed. The effects of β , ℓ and Λ on the photon regions have been discussed in our earlier paper, see Ref. 1. We do not repeat this here because there are no new qualitative aspects if α is present.

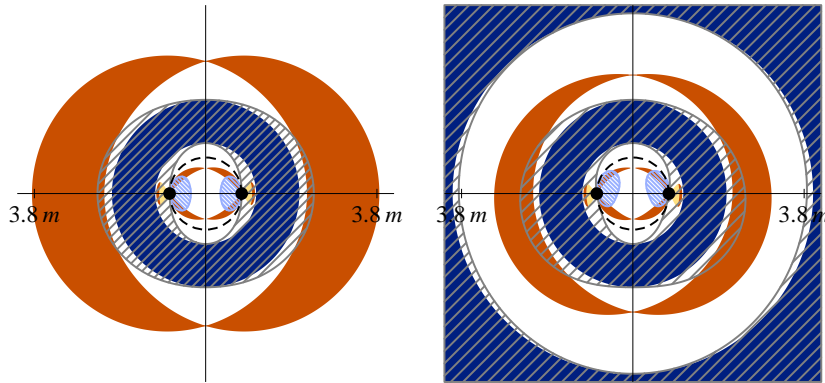


Fig. 3. Bigger versions of both plots shown in the fourth row of the third column in Fig. 2. Illustrated are the photon regions of spinning Kerr black holes ($a = \frac{4}{5}m$) where the left plot belongs to the ordinary space-time ($\alpha = 0$) and the right plot to an accelerated space-time ($\alpha = \frac{1}{4m}$).

4. Shadows of Black Holes

If one looks into the direction of a black hole then there is a region on the sky which stays dark, provided that there are no light sources between the observer and the black hole. This dark region is called the *shadow* of the black hole. To determine the shape of the shadow we consider light rays which are sent into the *past* from the

position (r_O, ϑ_O) of a fixed^b observer in the domain of outer communication. Then we can distinguish between two types of lightlike geodesics: Those where the radial coordinate increases after possibly passing through a minimum and those where the radial coordinate decreases until reaching the horizon at $r = r_+$. If we assume that there are light sources distributed in the universe, but not between the observer and the black hole, geodesics of the first kind could reach a light source; so we assign brightness to the initial direction of such a light ray. Correspondingly, we assign darkness to the initial directions of light rays of the second kind, i.e., these initial directions determine the shadow of the black hole. The boundary of the shadow corresponds to light rays on the borderline between the two kinds. These are light rays that spiral asymptotically towards one of the unstable spherical light orbits in the exterior photon region \mathcal{K} . Hence, the essential information for determining the shadow of a black hole is in the surrounding photon region. One may even say that the shadow is an image of the photon region (but not of the event horizon).

For deriving an analytical formula for the boundary curve of the shadow we proceed, again, as in the case without acceleration. First, we choose an orthonormal tetrad, cf. page 307 in Ref. 15, for our fixed observer at (r_O, ϑ_O)

$$\begin{aligned}
 e_0 &= \Omega \frac{(\Sigma + a\chi)\partial_t + a\partial_\varphi}{\sqrt{\Sigma\Delta_r}} \Big|_{(r_O, \vartheta_O)}, & e_2 &= -\Omega \frac{(\partial_\varphi + \chi\partial_t)}{\sqrt{\Sigma\Delta_\vartheta} \sin \vartheta} \Big|_{(r_O, \vartheta_O)}, \\
 e_1 &= \Omega \sqrt{\frac{\Delta_\vartheta}{\Sigma}} \partial_\vartheta \Big|_{(r_O, \vartheta_O)}, & e_3 &= -\Omega \sqrt{\frac{\Delta_r}{\Sigma}} \partial_r \Big|_{(r_O, \vartheta_O)}.
 \end{aligned} \tag{23}$$

Since our observer is in the domain of outer communication, Δ_r is positive. Σ is positive everywhere (except at the ring singularity which is not part of the space-time and, moreover, away from the domain of outer communication) and Δ_ϑ is positive by assumption. This guarantees real coefficients in Eqs. (23). It is easy to check that the e_i are orthonormal. As usual, the timelike vector e_0 is interpreted as the four-velocity of our observer. By our choice of the tetrad, $e_0 \pm e_3$ are tangential to the *principal null congruences* of our metric; e_3 points into the spatial direction towards the center of the black hole. So we have chosen the four-velocity of our observer adapted to the symmetries of the space-time in the sense that e_0 is in the intersection of the t - φ -plane and the plane spanned by the two principal null directions.

For any light ray $\lambda(s) = (r(s), \vartheta(s), \varphi(s), t(s))$, the tangent vector at the position of the observer can be written in two different ways, using either the coordinate basis or the tetrad introduced above,

$$\dot{\lambda} = \dot{r}\partial_r + \dot{\vartheta}\partial_\vartheta + \dot{\varphi}\partial_\varphi + \dot{t}\partial_t, \tag{24}$$

$$\dot{\lambda} = \sigma(-e_0 + \sin\theta \cos\psi e_1 + \sin\theta \sin\psi e_2 + \cos\theta e_3). \tag{25}$$

^bBecause of the symmetry, it is enough to specify the r and ϑ coordinate to define a fixed position in space-time.

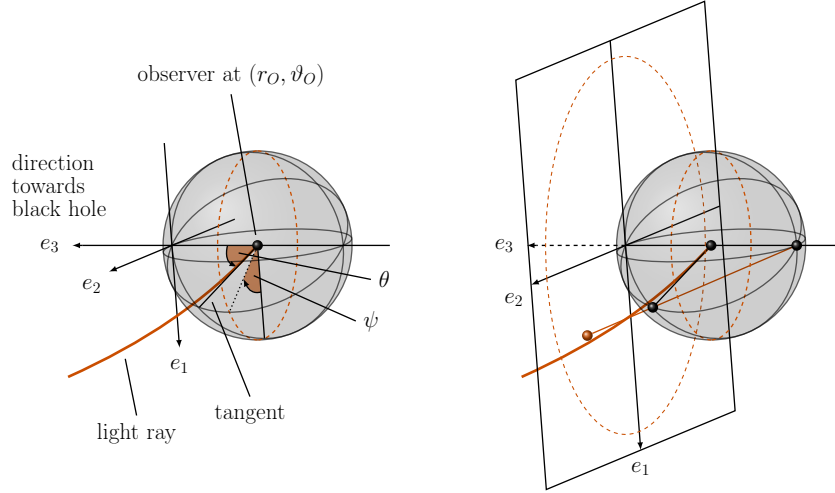


Fig. 4. Eq. (25) defines celestial coordinates θ and ψ for the light rays at the observer's position, as illustrated in the left figure. With this choice, $\theta = 0$ is the direction towards the black hole. Every direction of a light ray represented by a point (θ, ψ) on the celestial sphere (black ball) is visualized by its stereographic projection (red ball) on a plane. The dotted (red) circles are the celestial equator $\theta = \pi/2$ and its image under stereographic projection.

The second equation defines the celestial coordinates θ and ψ , see Fig. 4. For the scalar factor σ we obtain with (15)

$$\sigma = g(\dot{\lambda}, e_0) = \Omega \frac{aL_z - (\Sigma + a\chi)E}{\sqrt{\Sigma\Delta_r}} \Big|_{(r_O, \vartheta_O)}. \quad (26)$$

We substitute $\dot{\varphi}$ and \dot{r} from (16b) and (16d) into (24), and we insert the expressions of e_i from (23) into (25). Then comparing the coefficients of ∂_φ and ∂_r in the resulting two equations yields

$$T := \sin \theta = \frac{\sqrt{\Delta_r K_E}}{r^2 + \ell^2 - a\tilde{L}_E} \Big|_{r=r_O}, \quad (27a)$$

$$P := \sin \psi = \frac{\tilde{L}_E + a \cos^2 \vartheta + 2\ell \cos \vartheta}{\sqrt{\Delta_\vartheta K_E} \sin \vartheta} \Big|_{\vartheta=\vartheta_O}, \quad (27b)$$

where

$$\tilde{L}_E = L_E - a + 2\ell C. \quad (28)$$

If a light ray asymptotically approaches a spherical lightlike geodesic at a radius r_p in the photon region, it must have the same constants of motion as this limiting spherical geodesic. By (19) and (28), this implies that the constants of motion of light rays that correspond to boundary points of the shadow are given by

$$K_E(r_p) = \frac{16r^2 \Delta_r}{(\Delta_r')^2} \Big|_{r=r_p}, \quad a\tilde{L}_E(r_p) = \left(r^2 + \ell^2 - \frac{4r\Delta_r}{\Delta_r'} \right) \Big|_{r=r_p}. \quad (29)$$

Here the range of r_p is determined by the intersection of the exterior photon region (20) with the cone $\vartheta = \vartheta_O$, cf. Ref. 1. Thus, for a rotating black hole r_p ranges over an interval at whose boundary points (20) holds for $\vartheta = \vartheta_O$ with equality. If we insert (29) into (27), we get the boundary curve of the shadow on the observer's sky parametrized with r_p . In the case $a = 0$ the photon region degenerates into a photon sphere $r = r_p$. This unique value r_p defines a unique $K_E(r_p)$ but does not restrict \tilde{L}_E . Calculating the corresponding θ from (27) gives the radius of the shadow which is circular in this case. We may use \tilde{L}_E as a parameter for the boundary curve, where \tilde{L}_E varies between the extremal values given by (16c) for $\Theta(\vartheta_O) = 0$.

Comparison with Ref. 1 shows that the formula (20) for the photon region as well as the formulas (27, 28, 29) for the boundary curve of the shadow are identical with those of the non-accelerated case. However, the metric functions (3) have now a more general meaning because they include the acceleration parameter.

Several properties of the shadow are preserved, even with the acceleration parameter added. A non-rotating black hole still has a circular shadow since (27a) depends on the unique $K_E(r_p)$ but not on \tilde{L}_E , so $\theta = \text{constant}$ in this case. As the acceleration parameter breaks the spherical symmetry, this is a non-trivial result. Furthermore, the shadow is still independent of the Manko-Ruiz parameter C which is relevant only in the case $\ell \neq 0$. As in the non-accelerated case, the shadow is always symmetric with respect to a horizontal axis, because (ψ, θ) and $(\pi - \psi, \theta)$ are determined by the same constants of motion K_E and \tilde{L}_E . Again, this is a non-trivial result because it is not implied by an underlying symmetry unless $\ell = 0$, $\alpha = 0$ and $\vartheta_O = \pi/2$.

It is to be emphasized that we have calculated the shape of the shadow for an observer with a particular four-velocity, adapted to the principal null directions of the space-time. For an observer in a different state of motion, the shadow is distorted by aberration. These aberration effects have been discussed in detail in Ref. 39. As the aberration formula maps circles onto circles, the statement that a non-rotating black hole produces a circular shadow is true for an observer in *any* state of motion.

Figures 5 and 6 comprise images of shadows for different space-times seen by an observer at $r_O = 3.8m$ with varying inclination ϑ_O . As explained in Fig. 4, we map the shadow onto a plane by stereographic projection. Standard Cartesian coordinates in that plane of projection are given by

$$\begin{pmatrix} x(\rho) \\ y(\rho) \end{pmatrix} = -2 \tan\left(\frac{1}{2}\theta(\rho)\right) \begin{pmatrix} \sin\psi(\rho) \\ \cos\psi(\rho) \end{pmatrix} \quad (30)$$

In Fig. 5 we show the shadow for accelerated Kerr space-times where we have chosen the same values for α and a as in Fig. 2. Here, the observer is fixed at Boyer-Lindquist coordinates $r_O = 3.8m$ and $\vartheta_O = \pi/2$ (in the domain of outer communication). The different values of α are encoded into different shadings.

Also with acceleration, the shape of the shadow is largely determined by the spin a of the black hole. Hence, the shadow becomes more and more asymmetric with respect to a vertical axis with increasing spin a where the asymmetry results

16 Arne Grenzebach, Volker Perlick, Claus Lämmerzahl

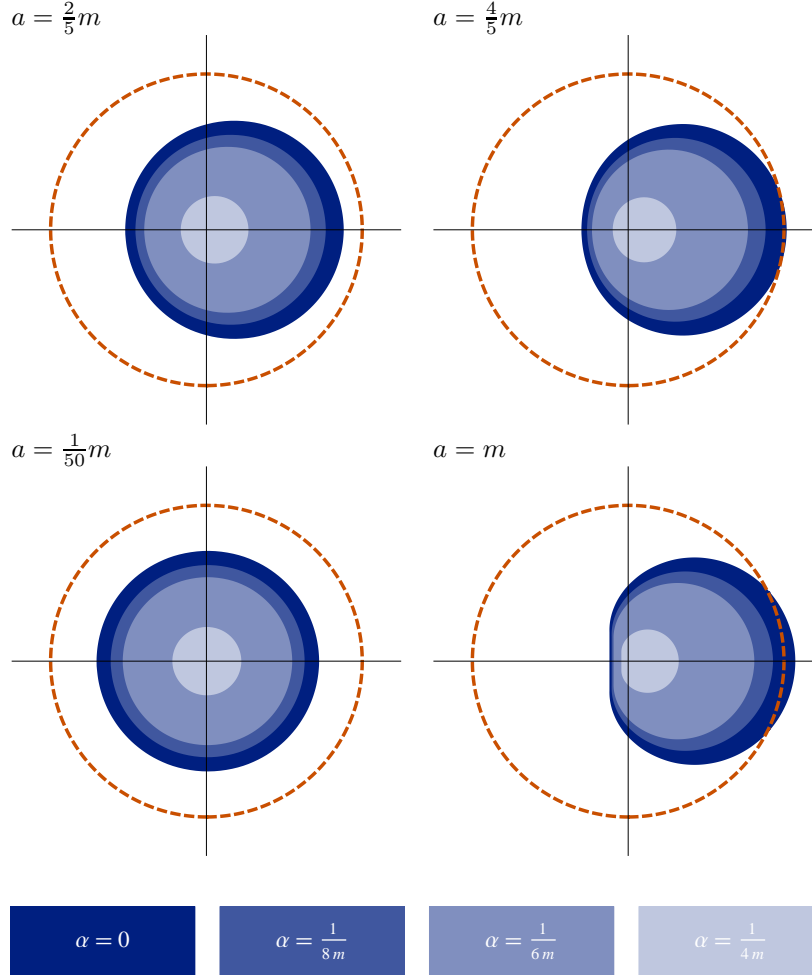


Fig. 5. Shadows of accelerated Kerr black holes ($a_{\max} = m$) seen by an observer at $r_O = 3.8m$ and $\vartheta_O = \pi/2$ for different spin values. The magnitude of the acceleration is color-coded where the specific values of α are listed below the plots. The dashed (red) circle marks the projection of the celestial equator, cf. Fig. 4.

from the “dragging effect” of the rotation on the light rays. The shadow is reflected at a vertical axis if the sign of a , i.e. the spin direction, is changed. One might have expected a similar effect with respect to a horizontal axis if the sign of α is changed. However, this is not true. As the shadow stays symmetric with respect to a horizontal axis even if $\alpha \neq 0$, the shadow is independent of the direction of the acceleration, i.e. of the sign of α . The acceleration has an effect on the *size* of the shadow, as is visible with the naked eye. This, however, has little relevance in view of observations because the size also scales with r_O and a comparison of the radius coordinates in different space-times has no direct operational meaning.

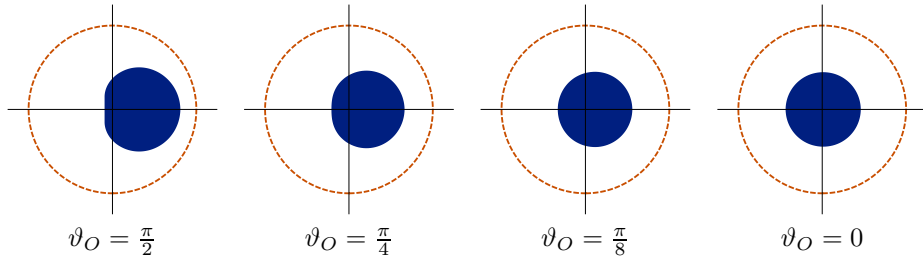


Fig. 6. Shadow of a black hole in accelerated Kerr space-time ($\alpha = \frac{1}{6m}$, $a = m = a_{\max}$) for an observer at $r_O = 3.8m$ with different inclination angles ϑ_O . As in Fig. 5, the dashed (red) circle indicates the celestial equator.

With the plots in Fig. 6 we investigate the influence of the observer's inclination ϑ_O on the shadow of an extremal Kerr black hole ($a = a_{\max} = m$) with acceleration $\alpha = \frac{1}{6m}$. As in Fig. 5 the observer is fixed at $r_O = 3.8m$. Clearly, for $\vartheta_O \rightarrow 0$ the shadow becomes circular. We have already emphasized the remarkable fact that the shadow is always symmetric with respect to the horizontal axis.

5. Angular Diameters of the Shadow of Black Holes

From the analytical formulas (27) and (29) for the boundary curve of the shadow we can deduce expressions for the horizontal and vertical angular diameters of the shadow. These correspond to the dashed lines in Fig. 7. Owing to the symmetry, the angular diameters δ_h and δ_v are determined by three angular radii ϱ_{h_1} , ϱ_{h_2} , and ϱ_v as indicated in Fig. 7,

$$\delta_h = \varrho_{h_1} + \varrho_{h_2}, \quad \sin \varrho_{h_i} = \sin \psi_{h_i} \sin \theta_{h_i} = P(r_{h_i})T(r_{h_i}), \quad (31)$$

$$\delta_v = 2\varrho_v, \quad \sin \varrho_v = \cos \psi_v \sin \theta_v = \sqrt{1 - P^2(r_v)}T(r_v), \quad (32)$$

where T and P have the same meaning as in (27).

In the following we restrict to the Kerr space-time with an observer in the equatorial plane, $\vartheta_O = \frac{\pi}{2}$. Even in this case, a formula for the angular diameters

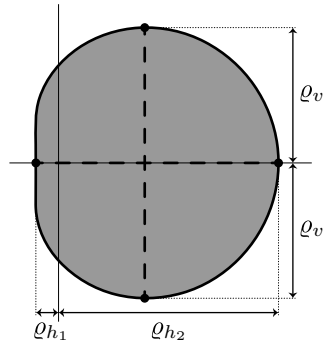


Fig. 7. Angular radii of the shadow of a black hole. Owing to the symmetry with respect to a horizontal axis, the two angular diameters (dashed lines) of the shadow are given by three angular radii: two horizontal radii ϱ_{h_i} and one vertical radius ϱ_v . The angular diameters are calculated as $\delta_h = \varrho_{h_1} + \varrho_{h_2}$ and $\delta_v = 2\varrho_v$, respectively.

18 *Arne Grenzebach, Volker Perlick, Claus Lämmerzahl*

of the shadow was not known before, as far as we know. In the general case, the angular diameters can be calculated analogously; it is true that then the radius values r_{h_i} and r_v are zeros of a polynomial of higher than fourth order, so they cannot be determined in closed form. In terms of these radii, however, one gets analytical formulas for the angular diameters also in the general case. The horizontal angular radii ϱ_{h_i} are characterized by $\psi_{h_i} = \pm \frac{\pi}{2}$, so we must solve the equation $1 = \sin^2 \psi(r_h) = P^2(r_h)$ which in the Kerr case simplifies to (use Eq. (27b) with Eq. (29))

$$r_h(r_h - 3m)^2 = 4ma^2 \quad (33)$$

$$\Rightarrow r_{h_1} = 2m + 2m \cos(\zeta/3), \quad (34a)$$

$$r_{h_2} = 2m - m \cos(\zeta/3) - \sqrt{3}m \sin(\zeta/3), \quad (34b)$$

$$r_{h_3} = 2m - m \cos(\zeta/3) + \sqrt{3}m \sin(\zeta/3), \quad (34c)$$

where $\zeta = \arg((2a^2m - m^3) - i(2am\sqrt{m^2 - a^2}))$. Here we have to choose the solutions r_{h_1} and r_{h_2} which are the radii of the two circular photon orbits in the exterior photon region. Evaluating PT for r_{h_1} and r_{h_2} yields by (31) the horizontal angular diameter δ_h of the shadow.

The vertical angular radius corresponds to those boundary points where the tangent is horizontal. By (32) we have $f(r_v) := \sin^2 \varrho_v = (1 - P^2(r_v))T^2(r_v)$, so the tangent is horizontal if $\frac{df}{dr_v}(r_v) = 0$. This yields

$$0 = (1 - P^2)T' - PP'T|_{r_v} \quad (35)$$

$$= \frac{\sqrt{\Delta(r_O)} r_v (r_v(2a^2 + r_O^2) - 3mr_O^2)(a^2m - r_v(3m^2 - 3mr_v + r_v^2))}{a^2 \sqrt{\Delta(r_v)} (r_v(2a^2 + r_O^2 + r_v^2) - m(r_O^2 + 3r_v^2))^2} \quad (36)$$

where we have to choose the unique solution inside the exterior photon region

$$r_v = \frac{3mr_O^2}{2a^2 + r_O^2}. \quad (37)$$

With this value r_v we get an analytic expression of the vertical angular radius

$$\sin^2 \varrho_v = (1 - P^2)T^2|_{r_v} = \frac{27m^2 r_O^2 (a^2 + r_O(r_O - 2m))}{r_O^6 + 6a^2 r_O^4 + 3a^2(4a^2 - 9m^2)r_O^2 + 8a^6}. \quad (38)$$

For $a = 0$, we recover from (38) Synge's formula²⁰ for a Schwarzschild black hole,

$$\sin^2 \varrho = \frac{27m^2(r_O - 2m)}{r_O^3}. \quad (39)$$

Since the shadow of a non-rotating black hole is always circular, the horizontal angular radii ϱ_{h_i} are also given by (39) in this case.^c Note that for all values $0 \leq a^2 \leq m^2$ (38) gives the same value as (39), $27m^2/r_O^2$, if m is negligibly small in

^cFor $a = 0$ one finds $\zeta = \arg(-m^3) = -\pi$ and $r_{h_{1,2}} = 3m$. Then $T^2(3m)$ reproduces (39).

comparison to r_O . This means that for observers far away from the black hole the vertical diameter of the shadow is independent of a .

In the extremal Kerr space-time, $a = m$, the circular photon orbits are at $r_{h_1} = 4m$ and $r_{h_2} = m$ since $\zeta = \arg(m^3) = 0$. Together with (37) this results in the following formulas for the angular radii

$$\begin{aligned} \sin^2 \varrho_{h_1} &= \frac{64m^2(r_O - m)^2}{(r_O^2 + 8m^2)^2}, & \sin^2 \varrho_v &= \frac{27m^2r_O^2}{(r_O + m)^2(r_O^2 + 8m^2)}. \\ \sin^2 \varrho_{h_2} &= \frac{m^2}{(r_O + m)^2}, \end{aligned} \quad (40)$$

Finally, we use (39) and (40) to determine the angular diameters given by (31) and (32) for the shadow of the black hole in the center of our Galaxy near Sgr A* and of that in M87. The resulting values are given in Table 1 together with the corresponding values for the mass M (in multiples of the Solar mass M_\odot) and the distance r_O of the black holes. We use two sets of parameters for M87 because the mass estimation based on the modeling of stellar dynamics yields a mass twice as big as the estimation based on gas dynamical measurements, compare Refs. 40–43.

The horizontal angular diameter for the extremal rotating black holes is always about 13% smaller than for the Schwarzschild case while the vertical angular diameters δ_v coincide in all cases. We have already observed that the latter is a consequence of the fact that r_O is large in comparison to m . It turns out that the shadow of the black hole in M87 is not much smaller than that of the black hole at the center of our Galaxy; the bigger distance of M87 is almost compensated by its bigger mass.

Table 1. Horizontal and vertical angular diameter δ_h , δ_v of the shadow for Sgr A* and M87 for a non-rotating Schwarzschild model ($a = 0$) or an extremal rotating Kerr model ($a = m$) of their black holes

	Sgr A*		M87		M87	
	δ_h	δ_v	δ_h	δ_v	δ_h	δ_v
$a = 0$	53.1 μas	53.1 μas	37.8 μas	37.8 μas	20.1 μas	20.1 μas
$a = m$	46.0 μas	53.1 μas	32.8 μas	37.8 μas	17.4 μas	20.1 μas
$m = \frac{MG}{c^2}$	$M = 4.31 \times 10^6 M_\odot$, $r_O = 8.33 \text{ kpc}^{5,6}$		$M = 6.2 \times 10^9 M_\odot$, $r_O = 16.68 \text{ Mpc}^{40-42}$		$M = 3.5 \times 10^9 M_\odot$, $r_O = 17.9 \text{ Mpc}^{40,43}$	

6. Conclusions and Outlook

We have seen that knowing the photon region surrounding a black hole is essential for calculating the shadow. For both the photon region and the boundary curve of the shadow we have found analytical formulas in the general type D class of Plebański–Demiański space-times. Since these space-times are not in general asymp-

totically flat and possess additional cosmological horizons, it is not possible to restrict to observers at infinity as it was done in many other articles on shadows of black holes. We have placed our observer at any Boyer–Lindquist coordinates in the outer domain of communication instead, and we have calculated the shadow for the case that the four-velocity of the observer is adapted to the symmetries of the space-time in the sense that it lies in the intersection of the t - φ -plane with the plane spanned by the principal null directions. Interestingly, for such an observer the shadow is always symmetric with respect to a horizontal axis, independently of an acceleration $\alpha \neq 0$, an inclination $\vartheta_O \neq \pi/2$ of the observer, or a gravitomagnetic NUT charge $\ell \neq 0$. The boundary curve of the shadow depends on the space-time parameters m , a , ℓ , β , α , and Λ , as well as on the observer’s position (r_O, ϑ_O) . For an observer whose four-velocity is not adapted to the symmetries of the space-time, the boundary curve of the shadow also depends on the 3 components of the spatial velocity with respect to our standard observer.

Although the acceleration parameter does not destroy the symmetry of the shadow with respect to a horizontal axis, it does have such an effect on the photon region, the ergosphere and the causality violating region. The photon region is reflected at the equatorial plane if the sign of α is changed whereas the ergoregion and the causality violating region are reflected at the equatorial plane if the sign of $a\alpha$ is changed.

Our estimates of the angular diameters for the shadows of the black holes in the centers of our Galaxy and of M87 show that the shadows are roughly of the same size. Hence the planned observations may provide us with shadow images not only of the black hole in our Galaxy but also of that in M87. If the current attempts of observing the shadow are successful, this will give us a chance to deduce the parameters of the black hole from the boundary curve of the shadow. Our analytical formula combined with a Fourier analysis should be a promising tool for achieving this goal. We are planning to investigate this in a follow-up article.

Acknowledgments

Our thanks for helpful discussions go to Nico Giulini, Norman Gürlebeck, David Kofron, Eva Hackmann, and Eugen Radu. We gratefully acknowledge support from the DFG within the Research Training Group 1620 “Models of Gravity”.

References

1. A. Grenzebach, V. Perlick, and C. Lämmerzahl, *Phys. Rev. D* **89** (2014) 124004
2. O. James, E. v. Tunzelmann, P. Franklin, K. S. Thorne, *Class. Quantum Grav.* **32** (2015) 065001
3. S. S. Doeleman *et al.*, *Nature* **455** (2008) 78
4. A. Eckart and R. Genzel, *Nature* **383** (1996) 415
5. S. Gillessen *et al.*, *Astrophys. J.* **692** (2009) 1075
6. A. M. Ghez *et al.*, *Astrophys. J.* **689** (2008) 1044

7. L. Huang, M. Cai, Zh.-Q. Shen, and F. Yuan, *Month. Not. R. Astron. Soc.* **379** (2007) 833
8. H. Falcke, F. Melia, and E. Agol, *Astrophys. J.* **528** (2000) L13
9. N. S. Kardashev, I. D. Novikov, V. N. Lukash, S. Pilipenko, et. al., *Uspekhi Fizicheskikh Nauk* **184** (2014) pp. 1319, english transl. *arXiv:1502.06071*
10. T. Levi-Civita, *Rend. Accad. Lincei* **28(1)** (1919) pp. 3
11. H. Weyl, *Ann. Physik* **54 (359)** (1917) pp. 117
12. H. Weyl, *Ann. Physik* **59 (364)** (1919) pp. 185
13. J. Ehlers and W. Kundt, Exact Solutions of the Gravitational Field Equations, in *Gravitation: an introduction to current research*, ed. L. Witten (John Wiley & Sons, New York, 1962), chp. 2
14. K. Hong and E. Teo, *Class. Quantum Grav.* **22** (2005) pp. 109
15. J. B. Griffiths and J. Podolský, *Exact Space-Times in Einstein's General Relativity*, (Cambridge University Press, Cambridge, 2009)
16. K. Hong and E. Teo, *Class. Quantum Grav.* **20** (2003) pp. 3269
17. W. Kinnersley and M. Walker *Phys. Rev. D* **2** (1970) pp. 1359
18. W. B. Bonnor, *Gen. Rel. Grav.* **15** (1983) pp. 535
19. W. B. Bonnor and W. Davidson, *Class. Quantum Grav.* **9** (1992) pp. 2065
20. J. L. Synge, *Mon. Not. R. Astron. Soc.* **131** (1966) 463
21. J. M. Bardeen, in *Black Holes (Les Astres Occlus)*, eds. C. DeWitt and B. S. DeWitt (Gordon and Breach, New York, 1973), p. 215
22. K. Hioki and K.-I. Maeda, *Phys. Rev. D* **80** (2009) 024042
23. J. M. Bardeen and C. T. Cunningham, *Astrophys. J.* **183** (1973) 237
24. J.-P. Luminet, *Astron. Astrophys.* **75** (1979) 228
25. J. Dexter, E. Agol, P. C. Fragile, and J. C. McKinney, *J. Phys.: Con. Ser.* **372** (2012) 012023
26. Z. Younsi, K. Wu, and S. V. Fuerst, *A&A* **545** (2012) A13
27. M. Mościbrodzka, H. Falcke, H. Shiokawa, and C. F. Gammie, *A&A* **570** (2014) A7
28. M. Mościbrodzka, H. Shiokawa, C. F. Gammie, and J. C. Dolence, *Astrophys. J. Lett.* **752** (2012) L1
29. J. Dexter and P. C. Fragile, *Mon. Not. R. Astron. Soc.* **432** (2013) 2252
30. R. Debever, *Bull. Soc. math Belgique* **23** (1971) 360
31. J. F. Plebański and M. Demiański, *Ann. Phys.* **98** (1976) 98
32. H. Stephani, D. Kramer, M. MacCallum, C. Hoenselaers, E. Herlt, *Exact Solutions of Einstein's Field Equations*, (Cambridge University Press, Cambridge, 2003)
33. A. N. Aliev and A. E. Gümrükçüoğlu, *Phys. Rev. D* **71** (2005) 104027
34. V. S. Manko and E. Ruiz, *Class. Quantum Grav.* **22** (2005) 3555
35. J. F. Plebański, *Ann. Phys.* **90** (1975) 196
36. B. Carter, *Commun. Math. Phys.* **10** (1968) 280
37. V. Perlick, *Living Rev. Relativ.* **7** (2004) 9
38. B. O'Neill, *The Geometry of Kerr Black Holes* (A K Peters, Wellesley, 1995)
39. A. Grenzebach, Aberrational Effects for Shadows of Black Holes, to appear in *Proc. 524th WE-Heraeus-Seminar "Equations of Motion in Relativistic Gravity"*, eds. D. Puetzfeld, C. Lämmerzahl, B.F. Schutz (Springer, Heidelberg, 2015)
40. A. Broderick, R. Narayan, J. Kormendy, et al., The Event Horizon of M87, submitted to *Astrophys. J.*
41. J. Kormendy and L. C. Ho, *Annu. Rev. Astron. Astrophys.* **51** (2013) 511
42. K. Gebhardt, J. Adams, D. Richstone, et al., *Astrophys. J.* **729** (2011) 119
43. J. L. Walsh, A. J. Barth, L. C. Ho, and M. Sarzi, *Astrophys. J.* **770** (2013) 86